Available on the CERN CDS information server

CMS PAS BPH-13-002

CMS Physics Analysis Summary

Contact: cms-pag-conveners-bphysics@cern.ch

2018/06/01

Measurement of production cross sections times branching fraction of $B_c^+ \to J/\psi\pi^+$ and $B^+ \to J/\psi K^+$ in pp collisions at $\sqrt{s} = 7$ TeV at CMS

The CMS Collaboration

Abstract

Measurements of the differential production cross section times branching fraction of the $B_c^+ \to J/\psi\pi^+$ and $B^+ \to J/\psi K^+$ processes are presented as a function of the $B_c^+(B^+)$ transverse momentum p_T and absolute rapidity $|y|$. The measurements are based on data collected by CMS in 2011 in pp collisions at $\sqrt{s} = 7$ TeV, corresponding to an integrated luminosity of 4.77 fb^{-1}. The integrated production cross sections times branching fraction in the kinematic region of $p_T(B_c^+,\ B^+) > 10$ GeV/c and $|y|(B_c^+,\ B^+) < 1.5$ are measured to be 40.8 ± 4.7 (stat.) $\pm$ 2.8 (syst.) pb for $B_c^+ \to J/\psi\pi^+$ and $5851.3 \pm 37.1 \pm$ (stat.) $\pm$ 446.4 (syst.) pb for $B^+ \to J/\psi K^+$. The $B^+ \to J/\psi K^+$ production is found to be described reasonably well by FONLL theoretical calculations, while the shape of $B_c^+ \to J/\psi\pi^+$ production is described well by BCVEGPY theoretical predictions.

1 Introduction

The $B_c^+(B_c^-)$ meson is a ground state of the $\overline{b}c(b\overline{c})$ system and contains two heavy quarks of different flavors, $\overline{b}$ and c quarks. The $\overline{b}c$ system is an intermediate state between the charmonium and bottonium systems. Being the carrier of the two different flavors, it provides ground for the study of heavy-quark dynamics which is different from those provided by $c\overline{c}$ and $b\overline{b}$ quarkonia. In the standard model, B^+ $(u\bar{b})$ is the b-quark meson with the largest production rate in hadron collisions whereas the production of the B_c^+ is rarer because it needs simultaneous production of $b\bar{b}$ and $c\bar{c}$ pairs. The study of heavy quark production in high energy hadronic interactions plays a critical role in testing next-to-leading order (NLO) Quantum Chromodynamics (QCD) calculations [1, 2] and more recent predictions by fixed order plus next-to-leading-logarithms (FONLL) [3, 4]. However, the dependence of the theoretical predictions on the renormalization and factorization scales and the b-quark mass m_b results in theoretical uncertainties up to 40%. Effective models inspired by QCD [5] have been developed for the B_c^+ meson for two decades. The complete order-α^4 approach [6–15] (where α is the strong-interaction coupling) predicts the B_c^+ production to be 0.2% of the inclusive $b\bar{b}$ cross section.

The first heavy quark production measurements were performed by the UA1 collaboration at the S$p\bar{p}$S (CERN) at a center-of-mass energy of $\sqrt{s} = 630$ GeV [16, 17]. Then the CDF and D0 collaborations at the Fermilab Tevatron measured heavy quark production at $\sqrt{s} = 1.8$ TeV and 1.96 TeV [18–25] and observed the B_c^+ in the semileptonic channel $B_c^+ \to J/\psi l^+ \nu$ and hadronic channel $B_c^+ \to J/\psi\pi^+$ [26–29]. After 2010, experiments at the Large Hadron Collider (LHC) achieved substantial progress in the understanding of heavy quark production. The LHCb collaboration has measured the relative production cross sections of b hadrons and B_c^+ in the forward rapidity region [30–34]. The CMS collaboration has measured the production cross sections for B^+, B^0, B_s, Λ_b, inclusive b hadron production and relative B_c^+ productions [35–42]. ATLAS has measured the B^+ and b hadrons production cross sections [43–45] and the measurement shows different transverse momentum and rapidity dependencies compared with predictions of the NLO MC generators(MCNLO+HERWIG) [45]. However, only the relative production ratios of B_c^+ to B^+ or B_s^0 cross sections have been measured at LHCb and CMS. The B^+ production measurement also serves as a standard candle for the B_c^+ production measurement. Therefore, precise measurements of the B^+ and B_c^+ cross sections times branching fraction at CMS will provide useful information on the production mechanism of B^+ and B_c^+ mesons. In this paper, the measurements of the production cross section times branching ratio of $B_c^+ \to J/\psi\pi^+$ and $B^+ \to J/\psi\, K^+$ at 7 TeV center of mass energy are reported as a function of b hadron transverse momentum p_T and rapidity $|y|$. Using the large $B^+ \to J/\psi K^+$ sample, the differential cross section $d\sigma/dp_T(B^+)$ ×BR for small and large rapidity events are investigated separately. The inclusion of charge conjugate modes is implied throughout this paper. The results are compared with the theoretical predictions based on QCD.

2 CMS detector and data sample

The central feature of the CMS apparatus is a superconducting solenoid of 6 m internal diameter, providing a magnetic field of 3.8 T. Within the solenoid volume are a silicon pixel and strip tracker, a lead tungstate crystal electromagnetic calorimeter, and a brass and scintillator hadron calorimeter, each composed of a barrel and two endcap sections. Muons are detected in gas-ionization chambers embedded in the steel flux-return yoke outside the solenoid. The silicon tracker and muon systems are the relevant subdetectors for the measurement described in this document. The silicon tracker, located in the 3.8 T magnetic field of the superconducting solenoid, is used to measure charged particles within the pseudorapidity range $|\eta| < 2.5$. It is composed of 66 million layers of $100 \times 150~\mu\text{m}^2$ silicon pixels and 9.6 million of silicon strips with pitches varying in the range from 80 to 183 μm.An efficient muon system with detection planes made of drift tubes, cathode strip chambers, and resistive plate chambers is deployed for the reconstruction and identification of muons up to $|\eta| = 2.4$. The first level (L1) of the CMS trigger system, composed of custom hardware processors, uses information from the calorimeters and muon detectors to select the most interesting events in a fixed time interval of less than 4 μs. The High Level Trigger (HLT) processor farm further decreases the event rate from around 100 kHz to around 300 Hz, before data storage. The detailed Monte Carlo (MC) simulation of the CMS detector response is based on GEANT4. A detailed description of the CMS experiment can be found in Ref. [46].

This analysis has been performed with the data recorded by the CMS detector in 2011 LHC run corresponding to an integrated luminosity of 4.77 fb^{-1}. We used MC samples for the validation of the analysis strategy, to determine the reconstruction efficiencies and to investigate the source of different systematic uncertainties. The B_c^+ signal sample was generated by the dedicated event generator BCVEGPY through the dominant hard subprocess $gg \rightarrow B_c + b + \bar{c}$ [47, 49] . The B_c^+ decay, hadronization of two spectator quarks, initial state radiation (ISR) and final state radiation (FSR) were simulated by PYTHIA [48]. The B^+ MC samples were produced by PYTHIA.

3 Event reconstruction

The identification of the B_c^+ (B^+) $\rightarrow J/\psi\pi^+$ (K^+) decay proceeds through the reconstruction of $J/\psi \rightarrow \mu^+\mu^-$ and B_c^+ (B^+) $\rightarrow J/\psi\pi^+$ (K^+). To identify the events in which a J/ψ decays into two muons, we use double muon triggers where a dimuon vertex is found and required to be displaced from the interaction point (beamspot) in order to reject prompt J/ψ events (displaced trigger). The displaced trigger selection criteria are: $cos\alpha > 0.9$, where α represents the pointing angle between the dimuon momentum and the direction from the beamspot to the dimuon vertex in the transverse plane; $L_{xy}/\sigma_{L_{xy}} > 3$ to select long lived J/ψ's, where L_{xy} is the dimuon decay length and $\sigma_{L_{xy}}$ is the corresponding uncertainty. Muons are required to have opposite charges, $|\eta^\mu| < 2.2$ and $p_T^\mu > 4$ GeV$/c$. In addition the dimuon p_T must be greater than 6.9 GeV$/c$ and the distance of closest approach between the two muons must be < 0.5 cm. The χ^2 probability of fitting the two muons to a common vertex must be $> 15\%$. We keep all the J/ψ candidates that have an invariant mass within $\pm 120\,\text{MeV}/c^2$ of the PDG value [50].

To reconstruct the B_c^+ and the B^+ mesons, the selected J/ψ candidate is combined with a track to which pion or kaon mass is assigned. The pion (kaon) track selection criteria are: normalized $\chi^2 < 3$; number of hits in pixel and tracker detectors should be greater than 1 and 10; the track $p_T > 2.3$ GeV$/c$. The decay vertex is reconstructed using a kinematic vertex fit [51], which constrains the dimuon invariant mass to the nominal J/ψ mass.

The B_c^+ meson selection criteria have been optimized in the kinematic region $p_\text{T} > 10$ GeV$/c$ and $|y| < 1.5$ by maximizing the significance $(S/\sqrt{S+B})$ as a figure of merit, where S is the signal yield obtained from a Gaussian fit to the MC reconstructed events and B is the amount of background inferred from the $J/\psi\pi$ invariant mass sidebands in the data. The same selection criteria have been used for B^+ mesons. The resulting requirements are: the probability of the combined vertex and kinematic fit > 0.03; $cos\theta > 0.98$, where θ is the angle in the xy plane between the B_c^+ momentum vector and the position vector from the beam spot to the reconstructed secondary vertex. A requirement is also placed on the B_c^+ decay length significance

$L_{xy}/\sigma_{L_{xy}} > 4.0$, where L_{xy} is the projection of the vector $\vec{s}$ pointing from the beam spot to the secondary vertex onto the transverse momentum and $\sigma_{L_{xy}}$ is the corresponding uncertainty. In order to determine the best approach in cases where multiple B_c^+ candidates were identified, two comparison studies were carried out: the case in which all candidates were considered and the case where only the highest p_T candidate was selected. The difference in the signal yields was found to be 2.9% (0.7%) for B_c^+ and 3.7% (1.5%) for B^+ in data (MC) samples. Due to the small differences in the yield, we keep all $B_c^+(B^+)$ passing candidates in both data and MC samples.

Figure 1 (left) shows the $J/\psi\ \pi^\pm$ invariant mass distribution for data after applying all the selection criteria. The B_c^+ signal is described by a Gaussian function. In the B_c^+ inclusive bin ($p_T > 10\ GeV/c; |y| < 1.5$), the Gaussian width and the mean are allowed to float in the fit. For the B_c^+ differential bins, the Gaussian width is allowed to float while the mean value is fixed to the best fit value of the inclusive bin. The background is described by a 2^{nd} order Chebyshev polynomial function. The fitted yield for $B_c^\pm$ is 310 ± 36 and the mass extracted from the fit is 6272.5 ± 2.9 MeV/c^2, consistent with the PDG average value [50].

Figure 1 (right) shows the $J/\psi\ K^\pm$ invariant mass distribution. The B^+ signal is described by the sum of three Gaussian functions. In the B^+ inclusive bin ($p_T > 10\ GeV/c; |y| < 1.5$), the width and the mean of the Gaussian function are allowed to float in the fit. For the B^+ differential bins, the width of the Gaussian functions are allowed to float while the mean is fixed to the value of the inclusive bin. The background is parametrized by the combination of an exponential function (for the combinatorial contribution) and a Gaussian which describes the partially reconstructed $B^0 \to J/\psi K^*(892)$ as shown by dashed blue and dashed red line, respectively. The contribution of the $B^\pm \to J/\psi\pi^\pm$ process is modeled by a Gaussian function (shown in green), whose parameters values are extracted from MC simulation. The fitted yield for the $B^\pm$ is 117091 ± 347 and the mass extracted from the fit is 5279.36 ± 0.01 MeV/c^2, consistent with the PDG average value [50].

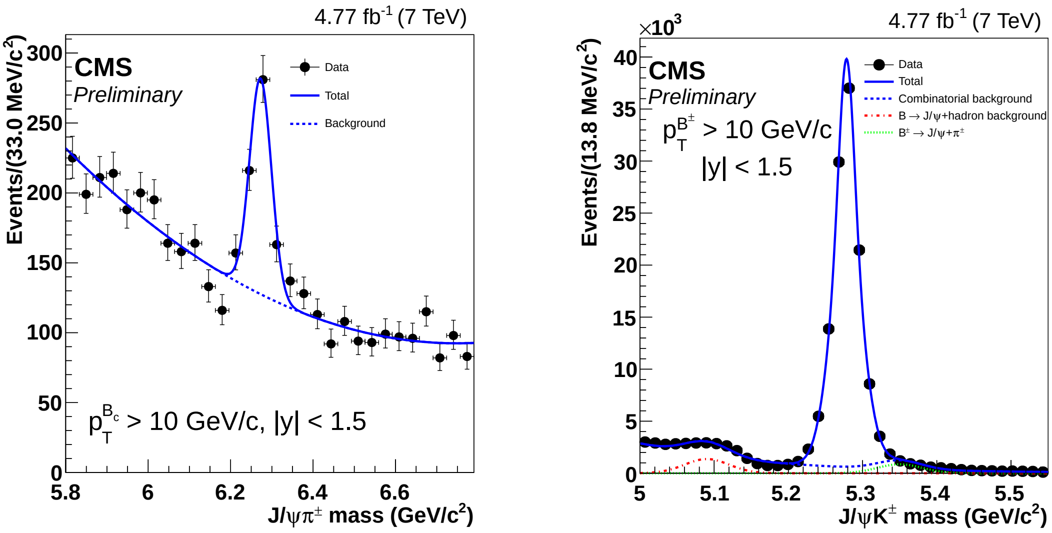

Figure 1: Invariant mass distribution of $J/\psi\pi^\pm$ (left) and $J/\psi K^\pm$ (right) for 2011 CMS data. The curves show the best maximum likelihood fit for the sample.

4 Measurement of the cross section times branching fraction

The $B_c^+ \to J/\psi\pi^+ (B^+ \to J/\psi K^+)$ production cross section times branching fraction is measured in p_T ($|y|$) bins by using the observed $B_c^+ (B^+)$ event yield corrected by the efficiency and data luminosity, as in Equation 1:

$$\frac{d\sigma(pp \to B_c^+ + X)}{dp_T(B_c^+)} \cdot \mathcal{B}(B_c^+ \to J/\psi\pi^+) = \frac{N_{sig}}{2 \cdot \epsilon \cdot \mathcal{B}(J/\psi \to \mu\mu) \cdot \Delta p_T(B_c^+) \cdot \mathcal{L}}, \quad (1)$$

where $\mathcal{L}$ is the integrated luminosity of the dataset, N_{sig} is the observed number of the $B_c^+ (B^+)$ candidates extracted by performing an unbinned extended maximum-likelihood fit to the invariant mass distribution of the candidates in the given p_T or $|y|$ bin, $\mathcal{B}(J/\psi \to \mu\mu) = (5.961 \pm 0.033)\%$ is obtained from PDG [50] and Δp_T ($|y|$) is the bin width. The factor of 2 accounts for our choice of quoting the $B_c^+ (B^+)$ cross section times branching fraction for positive charge only while N_{sig} includes both B_c^+ and B_c^-. We used the same expression as in Equation 1 for the differential cross section measurement as a function of $|y|$. To get the B_c^+ differential cross section times branching fraction, we separated the selected events into three bins with respect to p_T and $|y|$ as listed in Table 1, while for B^+ the measurement has been performed in nine p_T and $|y|$ bins as listed in Table 2. The analysis also includes 2D differential cross section times branching fraction of B^+, which has been performed in five p_T bins for $0.0 < |y| < 0.75$ and $0.75 < |y| < 1.5$.

The total efficiencies (ϵ) for the $B_c^+ \to J/\psi(\mu^+\mu^-)\pi^+$ and $B^+ \to J/\psi(\mu^+\mu^-)K^+$ processes are computed as the product of acceptance (Acc.), reconstruction efficiency ($\epsilon_{reco.}$) and scale factors for muon and displaced trigger efficiencies (α_μ *and* α_{Disp}) used in order to cover the discrepancy between corresponding efficiencies in data and MC, as expressed below:

$$\epsilon = Acc. \cdot \epsilon_{reco.} \cdot \alpha_\mu \cdot \alpha_{Disp}. \quad (2)$$

The acceptance and reconstruction efficiencies are calculated using simulated events for the $B_c^+ \to J/\psi(\mu^+\mu^-)\pi^+$ and $B^+ \to J/\psi(\mu^+\mu^-)K^+$ processes. The acceptance is mainly determined by the dimuon detection coverage of CMS and is defined as:

$$Acc. = \frac{N_{gen}(p_T(J/\psi) > 6.9\ GeV/c), \mu(acc.))}{N_{gen}}, \quad (3)$$

where $\mu(acc.)$ are the muon acceptance requirements listed in the event reconstruction section and N_{gen} is the total number of generated events with $p_T(B_c^+,\ B^+) > 10$ GeV/c and $|y|$ $(B_c^+,\ B^+) < 1.5$.

The reconstruction efficiency is defined as:

$$\epsilon_{reco.} = \frac{N_{kin.}^{acc.}}{N^{acc.}}, \quad (4)$$

where $N^{acc.}$ is the total number of events passing acceptance criteria as in Equation 3 and $N_{kin.}^{acc.}$ is the total number of selected events after reconstruction.

To determine α_μ, the single muon tracking, identification and trigger efficiencies were measured individually by using prompt J/ψ data and MC samples as a function of the $p_T(\mu)$ and $|y|$ bins by the Tag-and-Probe technique and were translated to $p_T(B_c^+,\ B^+)$ and $|y|$ bins. The dimuon efficiency is calculated by the product of single muon efficiencies, i.e. $\epsilon_{D\mu} = \epsilon_{\mu_1} \times \epsilon_{\mu_2}$. The dimuon efficiency is calculated on an event-by-event basis similarly to the reconstruction efficiency and acceptance. The total muon efficiency is computed over all events in a particular p_{T} and pseudorapidity range, as illustrated in Equation 5:

$$\epsilon_{\mu}^{tot.}(p_T\ (B_c^+),\ |y|(B_c^+)) = N(p_T\ (B_c^+),\ |y|(B_c^+)) / \sum_{i=0}^{i=N(p_T(B_c^+),\ |y|(B_c^+))} \frac{1}{\epsilon_{D\mu,\ i}}, \quad (5)$$

where $N(p_T, |y|)$ is the number of signal events in the particular $B_c^+(B^+)$ p_T or $|y|$ bin. The scale factor for muon efficiency, α_{μ}, is then calculated by the ratio of total muon efficiency in data and MC samples. The discrepancy between the muon efficiency in data and MC decreases with an increase in p_{T} and α_{μ} varies between 0.90 to 0.93 for B_c^+, between 0.86 to 0.97 for B^+ in different p_{T} and $|y|$ bins.

The scale factor for the displaced trigger efficiencies, α_{Disp}, is calculated by the ratio between the relative displaced trigger efficiency as measured in data and MC. The displaced trigger efficiency is measured with respect to a dimuon trigger without requirements on the dimuon vertex position. The α_{Disp} is estimated to be varying between 1.010 to 1.013 for B_c^+ and ranges from 0.96 to 0.98 for B^+ in different p_{T} and $|y|$ bins.

5 Systematic uncertainties

The main sources of systematic uncertainty on the cross section times branching fraction measurements are uncertainties on the modeling of the mass shape, on tracking efficiencies of hadrons and muons, uncertainties in the detector alignment and in the integrated luminosity calculation. The systematic uncertainties taken into account are described below.

- Uncertainties on signal shape:
  Biases introduced by the modeling of the signal shape are calculated as the difference in signal yield per (p_{T},$|y|$) bin when fitting the B_c^+ mass spectrum with either a Gaussian or Crystal Ball function, where the width of both is allowed to float in the fit. Likewise, the B^+ signal yield and shape uncertainty is determined by the difference of signal yield per (p_{T},$|y|$) bin when fitting B^+ mass spectrum with the sum of two or three Gaussian functions, letting the widths float freely. The uncertainty on the signal shape was found to be 0.1% for B_c^+ and varying between 0.1-0.4% for B^+ for inclusive and differential bins.
- Uncertainties on background shape:
  The uncertainty affecting the "background shape" for B_c^+ is taken as the difference in signal yield per (p_{T},$|y|$) bin when fitting the background with a Chebyshev polynomial or an exponential function keeping the same signal model. Likewise, the B^+ background shape and yield uncertainty is determined by fitting the background with the combination of either a Gaussian and exponential function or a crystal Ball function and 2^{nd} order Chebyshev polynomial. The uncertainty on the background shape was found to be varying between 0.2-1.4% for B_c^+ and 0.2-1.0% for B^+ for inclusive and differential bins.
- Uncertainty on p_{T}($|y|$) binning:
  For differential measurements, the uncertainty due to the energy scale is a non-negligible effect that describes how B_c^+ (B^+) events migrate from a given p_{T}($|y|$) bin at generator level to a given bin at the reconstruction level. To estimate this effect, the B_c^+ (B^+) reconstructed fitted events have been matched with the generator level events using the MC truth information for each p_{T} and $|y|$ bin. The difference in the

yields in each $p_T(|y|)$ is quoted as the uncertainty of the $p_T(|y|)$ binning varying from 0.1 to 0.6%.

- Statistical uncertainty of MC samples:
  The statistical uncertainty of the reconstruction efficiency ranges between 0.7-1.3% and 0.9-2.6%, evaluated for the B_c^+ and B^+ measurements, respectively.
- Statistical uncertainty of Tag-and-Probe samples:
  The statistical uncertainties of MC and data samples used to determine the muon related efficiencies using the Tag-and-Probe technique are found to be between 1.2-1.4% and 1.9-2.4% for the B_c^+ and B^+ measurements, respectively.
- Uncertainty on hadron tracking efficiency:
  The uncertainty on efficiency for reconstruction of a hadron track is 3.9%, as in [52].
- Uncertainty on muon kinematics:
  Due to limited statistics in the MC samples used in the Tag-and-Probe technique the average value of muon efficiency was used for each p_T and $|y|$ bin. To estimate the efficiency variance due to the difference of the muon kinematic distribution between the MC samples used for Tag-and-Probe and B_c^+ (B^+) signal MC samples, we re-weight the MC muon p_T distribution to describe the data. The difference of the efficiencies, determined by using the samples with and without re-weighting, is considered to be the uncertainty of muon kinematic distribution. This uncertainty varies from 0.1 to 1.5% for inclusive and differential bins of $B_c^+(B^+)$ measurements.
- Uncertainty on muon tracking:
  The uncertainty on muon tracking is taken to be 0.5% [52].
- Uncertainty on alignment:
  The uncertainty associated with alignment of the tracker is estimated by comparing the simulated events with distorted geometries. From this, uncertainties are assigned ranging from 2.6(1.6)% to 4.2(3.3)% for inclusive and differential bins of $B_c^+(B^+)$ measurements.
- Uncertainty on luminosity estimation:
  An uncertainty of 4% is assigned to the luminosity estimation [53].
- PU conditions:
  Possible systematic uncertainties due to different pileup conditions have been assessed by dividing the data into two independent samples based on the number of reconstructed primary vertices per event, and the statistical consistency of the cross section measurements performed on the subsets of data has been evaluated. In the B_c^+, the two sub-samples have been found statistically consistent, thus no systematics have been assigned. However, in the B^+, the systematic uncertainties due to PU conditions were found to be varying in the range from 0.0 and 8.4%.
- Uncertainty on candidate arbitration:
  A difference of 2.2% was observed in the MC and data yields while selecting all $B_c^+(B^+)$ candidates and the case where only the highest p_T candidate was selected in an event. This difference has been introduced as an uncertainty on the measurement.

6 Results

Using the number of observed B_c^+ (B^+) candidates and the total efficiencies, we get the values for the cross section times branching fraction of $B_c^+ \to J/\psi\pi^+$ and $B^+ \to J/\psi K^+$. The prediction of branching fraction of $\mathcal{B}(B_c \to J/\psi\pi)$ has a wide spread because of the calcu-

Table 1: Measurements of integrated and differential cross section times branching fraction for $p_T(B_c^+) > 10$ GeV/c and $|y| < 1.5$. The first uncertainties are statistical and the second are systematic. The branching ratio (BR) $\mathcal{B}(B_c \to J/\psi\pi)$, used to evaluate the prediction from BCVEGPY, is 3.3×10^{-3} [54].

$p_T(B_c^+)$	n_{sig}	ϵ	$d\sigma/dp_T(B_c^+) \times$BR (pb/ GeV)	BCVEGPY (pb/ GeV)
10-16	101.0 ± 23.0	0.0050 ± 0.0001	$5.48 \pm 1.25 \pm 0.42$	2.02
16-22	101.3 ± 18.1	0.0380 ± 0.0005	$0.77 \pm 0.14 \pm 0.06$	0.30
22-50	107.0 ± 18.1	0.1030 ± 0.0014	$0.06 \pm 0.01 \pm 0.01$	0.02
$\lvert y\rvert(B_c^+)$	n_{sig}	ϵ	$d\sigma/d\lvert y\rvert(B_c^+)\times$BR (pb)	BCVEGPY (pb)
0-0.5	99.6 ± 16.3	0.0122 ± 0.0001	$28.23 \pm 4.62 \pm 2.07$	10.20
0.5-0.9	101.6 ± 18.8	0.0139 ± 0.0002	$31.77 \pm 5.87 \pm 2.48$	9.91
0.9-1.5	99.3 ± 20.9	0.0137 ± 0.0002	$21.07 \pm 4.44 \pm 1.51$	9.03
	n_{sig}	ϵ	$\sigma\times$BR (pb)	BCVEGPY (pb)
inclusive	$309.68 + 35.78$	0.0132 ± 0.0001	$40.78 \pm 4.71 \pm 2.84$	14.48

lations performed using different models [54]. The predicted value of the branching fraction $\mathcal{B}(B_c^+ \to J/\psi\pi^+) = 3.3 \times 10^{-3}$ [54] has been used for the current measurement. The differential measurements $d\sigma(B_c^+)/dp_T(B_c^+) \times \mathcal{B}(B_c^+ \to J/\psi\pi^+)$ and $d\sigma(B_c^+)/d|y|(B_c^+) \times \mathcal{B}(B_c^+ \to J/\psi\pi^+)$ along with theoretical predictions based on BCVEGPY are listed in Table 1. Figure 2 summarizes the differential cross sections times branching fraction results as a function of the B_c^+ p_T (left) and $|y|$ (right). The integrated production cross section times branching fraction for $B_c^+ \to J/\psi\pi^+$ with $p_T(B_c^+) > 10$ GeV and $|y|(B_c^+) < 1.5$ is $(40.8 \pm 4.7 \pm 2.8)$ pb, where the first uncertainty is statistical and the second is systematic.

The theoretical predictions of the B_c^+ production cross section times branching fraction have large uncertainties for a number of reasons. The branching fraction $\mathcal{B}(B_c^+ \to J/\psi\pi^+)$ involves the non-perturbative $B_c^+ \to J/\psi X$ transition form factors, the QCD corrections for which are large [57, 59]. The QCD corrections may also provide sizable contributions to the production cross section. The generator BCVEGPY is based on tree-level calculations of the gluon-gluon fusion production mechanism, and only the color-singlet $1S$-wave and $1P$-wave B_c^+ states are considered. There is a scale factor of 2.75 between theory and experiment. There are large uncertainties from the choices of the quark masses and the renormalization and factorization scales [47, 49, 55, 56]. It is also found that an appropriate choice of renormalization scale can achieve better predictions. For example, it has been found that by using the optimal scale determined by using the principle of maximum conformality [60], one can get a better B_c^+ semileptonic decay width that agrees with the measurements [59]. The shape of the measurement shows consistency with the predictions from BCVEGPY as illustrated in Figure 2, where the prediction has been normalised to the measurement with a normalisation factor of 2.75.
Differential measurements $d\sigma(B^+)/dp_T(B^+) \times \mathcal{B}$ $(B^+ \to J/\psi K^+)$ and $d\sigma(B^+)/d|y|(B^+) \times \mathcal{B}(B^+ \to J/\psi K^+)$ have also been reported. The corresponding efficiency and cross section results are listed in Table 2 for differential p_T and $|y|$ bins. The integrated $\sigma(B^+) \times \mathcal{B}$ with $p_T(B^+) > 10$ GeV and $|y|(B^+) < 1.5$ is measured to be $5851.3 \pm 37.1 \pm 446.4$ pb, where the first uncertainty is statistical and second is systematic. The differential cross section times branching fraction for B^+ are also reported for $0.0 < |y| < 0.75$ and $0.75 < |y| < 1.5$ in five p_T bins. A comparison of the measurements with theoretical approaches (PYTHIA, FONLL and NLO) has

Table 2: Measurement of integrated and differential cross section times branching fraction for $p_{\mathrm{T}}(B^+) > 10$ GeV/c and $|y| < 1.5$. The first uncertainties are statistical and the second are systematic.

$p_T(B^+)$	n_{sig}	ϵ	$d\sigma/dp_T(B^+)\times$BR (pb / GeV)
10-14	14277.3 ± 128.1	0.0072 ± 0.0002	$864.03 \pm 14.25 \pm 74.68$
14-16	14752.0 ± 129.7	0.0363 ± 0.0009	$355.46 \pm 5.76 \pm 27.35$
16-18	15148.2 ± 121.5	0.0605 ± 0.0015	$218.68 \pm 3.27 \pm 15.91$
18-20	13612.1 ± 118.7	0.0851 ± 0.0022	$139.69 \pm 2.25 \pm 10.36$
20-22	11573.4 ± 111.8	0.1082 ± 0.0030	$93.46 \pm 1.65 \pm 6.92$
22-25	13493.9 ± 120.9	0.1347 ± 0.0035	$58.33 \pm 0.96 \pm 4.17$
25-29	12353.7 ± 110.3	0.1695 ± 0.0046	$31.85 \pm 0.52 \pm 3.58$
29-36	11596.1 ± 111.3	0.2129 ± 0.0058	$13.60 \pm 0.24 \pm 0.96$
36-120	10721.0 ± 109.3	0.2644 ± 0.0075	$0.84 \pm 0.02 \pm 0.06$
$\|y\|(B^+)$	n_{sig}	ϵ	$d\sigma/d\|y\|(B^+)\times$BR (pb)
0-0.15	12637.7 ± 113.2	0.0312 ± 0.0009	$4724.94 \pm 77.83 \pm 352.00$
0.15-0.3	12745.3 ± 116.4	0.0336 ± 0.0009	$4420.09 \pm 74.08 \pm 332.51$
0.3-0.45	12993.2 ± 116.5	0.0334 ± 0.0009	$4534.39 \pm 74.78 \pm 358.07$
0.45-0.6	13583.0 ± 119.0	0.0365 ± 0.0010	$4337.03 \pm 70.07 \pm 483.15$
0.6-0.75	13561.3 ± 120.8	0.0378 ± 0.0010	$4182.00 \pm 68.56 \pm 304.31$
0.75-0.9	12438.3 ± 117.6	0.0346 ± 0.0001	$4191.38 \pm 72.43 \pm 321.54$
0.9-1.05	11492.5 ± 247.0	0.0353 ± 0.0010	$3793.21 \pm 142.75 \pm 283.53$
1.05-1.25	14075.1 ± 126.3	0.0366 ± 0.0009	$3361.74 \pm 55.48 \pm 274.90$
1.25-1.5	14603.2 ± 133.6	0.0350 ± 0.0009	$2917.55 \pm 48.96 \pm 214.46$
	n_{sig}	ϵ	$\sigma\times$BR (pb)
inclusive	117091.38 ± 347.44	0.0351 ± 0.0003	$5851.34 \pm 37.09 \pm 446.39$

been made as shown in Figure 3, where the shaded region shows the theoretical uncertainty of 35%. In the case of FONLL and NLO, the calculations have been performed assuming a hadronization fraction of $f_{b\bar{b}\to B^+} = 0.337 \pm 0.002$. The FONLL B^+ cross section times branching fraction prediction is $4896.8^{+1667.6}_{-1086.7}$ $(scale) \pm 249.3$ $(mass)$ pb and includes uncertainties of b-quark mass, renormalization and factorization scales. In FONLL, the mass of the b-quark and the scales are set to be 4.75 ± 0.25 GeV$/c^2$ and $\mu_F = \mu_R = \mu_0$, respectively [58]. The uncertainties from renormalization scale (μ_0) and factorization scale (μ_R) are estimated by varying them up and down by a factor of two ($\mu_0/2 < \mu_R$, with $\mu_F < 2\mu_0; 1/2 < \mu_R/\mu_F < 2$) [58]. For estimating the b-quark mass uncertainty, the mass has been changed from 4.75 GeV$/c^2$ to 5.00 GeV$/c^2$ and 4.5 GeV$/c^2$ [58]. The theoretical predictions are in good agreement with the measurements within the theoretical uncertainties. The consistency of the measurements improves towards higher p_T and $|y|$. In this analysis, the ratio between $\sigma(B_c^+) \times \mathcal{B}(B_c^+ \to J/\psi\pi^+)$ and $\sigma(B^+) \times \mathcal{B}(B^+ \to J/\psi K^+)$ has also been measured and found to be 0.0049 ± 0.0006, consistent with CMS results in reference [42]. The B^+ cross section measurement has also been extracted for common phase space ($13 < p_T < 120$, $|y| < 1.5$) with the ATLAS measurement [45]. The result, 163.1 ± 2.27 $(stat.) \pm 9.13$ $(sys.) \pm 6.5$ $(lumi.)$ pb, is found to be consistent with the ATLAS measurement of 185.6 ± 5.28 $(stat.) \pm 12.3$ $(syst) \pm 3.5$ $(lumi.)$, within the total uncertainties by both experiments.

7 Summary

The production cross section times branching fractions $\sigma(B_c^+) \times \mathcal{B}(B_c^+ \to J/\psi\pi^+)$ and $\sigma(B^+) \times \mathcal{B}(B^+ \to J/\psi K^+)$ are measured at CMS. The measurement uses a dataset collected by the CMS detector in 2011 at $\sqrt{s} = 7$ TeV, which corresponds to an integrated luminosity of 4.77 fb^{-1}. The differential measurements $d\sigma(B_c^+) \times \mathcal{B}(B_c^+ \to J/\psi\pi^+)$ and $d\sigma(B^+) \times \mathcal{B}(B^+ \to J/\psi K^+)$ are reported with respect to $p_T(B_c^+,\ B^+)$ and rapidity $|y|$. The shape of $\sigma(B_c^+) \times \mathcal{B}(B_c^+ \to J/\psi\pi^+)$ measurement has been compared with the normalised theoretical predictions based on BCVEGPY and is found to be in good agreement. The $\sigma(B^+) \times \mathcal{B}(B^+ \to J/\psi K^+)$ measurements have also been compared with the predictions based on PYTHIA, FONLL and NLO calculations. The predictions from the NLO and FONLL theoretical framework have also been quoted with the theoretical uncertainty from the renormalization and factorization scale and b-quark mass (35%). The measurements are found to be consistent with the theoretical predictions within uncertainty. We hope the measurements may be helpful for theorists to understand and investigate the B_c^+ and B^+ production and decay mechanism further.

We congratulate our colleagues in the CERN accelerator departments for the excellent performance of the LHC machine. We thank the technical and administrative staff at CERN and other CMS institutes, and acknowledge support from: FMSR (Austria); FNRS and FWO (Belgium); CNPq, CAPES, FAPERJ, and FAPESP (Brazil); MES (Bulgaria); CERN; CAS, MoST, and NSFC (China); COLCIENCIAS (Colombia); MSES (Croatia); RPF (Cyprus); MoER, SF0690030s09 and ERDF (Estonia); Academy of Finland,MEC, andHIP (Finland); CEAand CNRS/IN2P3 (France); BMBF, DFG, andHGF (Germany); GSRT (Greece); OTKA andNKTH(Hungary); DAE and DST (India); IPM (Iran); SFI (Ireland); INFN (Italy); NRF and WCU (Korea); LAS (Lithuania); CINVESTAV, CONACYT, SEP, and UASLP-FAI (Mexico); MSI (New Zealand); PAEC (Pakistan); MSHE and NSC (Poland); FCT (Portugal); JINR (Armenia, Belarus, Georgia, Ukraine, Uzbekistan); MON, RosAtom, RAS and RFBR (Russia); MSTD (Serbia); SEIDI and CPAN (Spain); Swiss Funding Agencies (Switzerland); NSC (Taipei); TUBITAK and TAEK (Turkey); STFC (United Kingdom); DOE and NSF (USA).

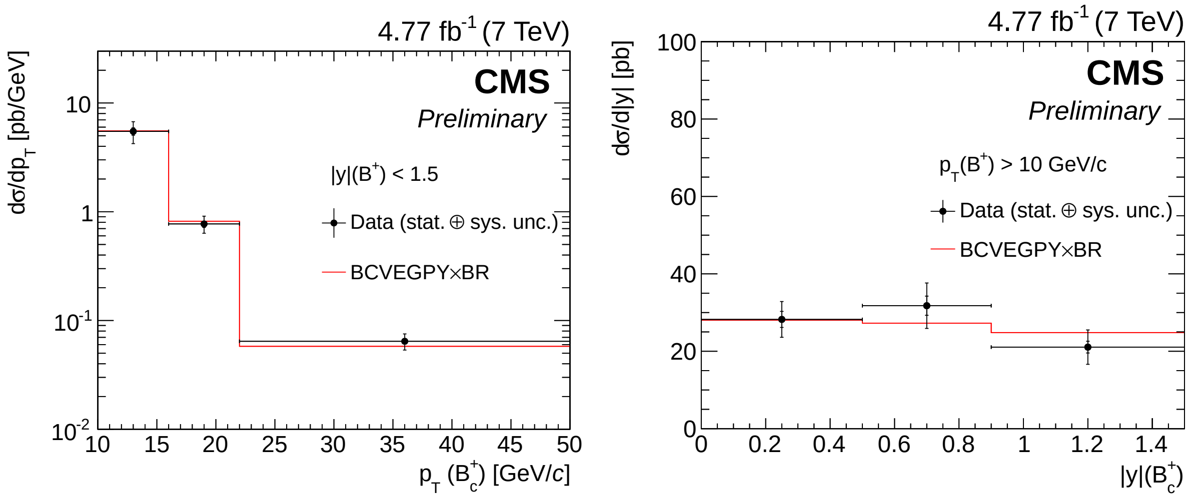

Figure 2: Differential production cross sections×BR of $d\sigma(B_c^+)/dp_T(B_c^+) \times \mathcal{B}(B_c^+ \to J/\psi\pi^+)$ (left) and $d\sigma(B_c^+)/d|y|(B_c^+) \times \mathcal{B}(B_c^+ \to J/\psi\pi^+)$ (right) at $\sqrt{s}$= 7 TeV pp collisions. Solid points with error bars are the CMS measurements and the uncertainties are statistical and systematic, respectively. The prediction of the B_c^+ production cross section by BCVEGPY times the branching fraction $\mathcal{B}(B_c \to J/\psi\pi) = 3.3 \times 10^{-03}$ [54] is scaled by 2.75 for display purposes.

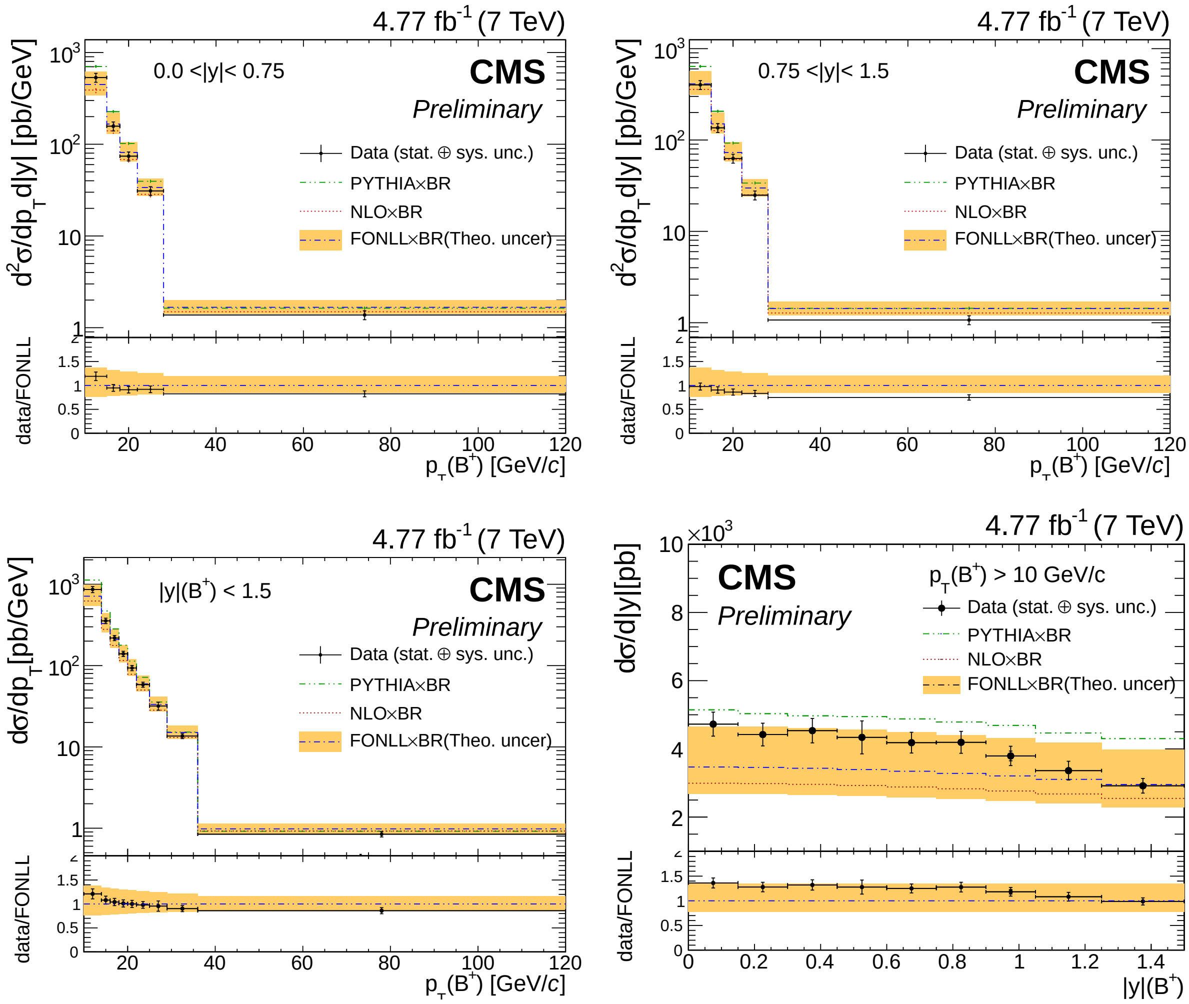

Figure 3: Top: Differential production cross sections $d\sigma/dp_{\mathrm{T}} \times \mathcal{B}(B^+ \rightarrow J/\psi K^+)$ for $B^+ \rightarrow J/\psi K^+$ at $\sqrt{s}$= 7 TeV pp collisions for $0.0 < |y|(B^+) < 0.75$ (left) and $0.75 < |y|(B^+) < 1.5$ (right). Solid points with error bars are the CMS measurements and the uncertainties are statistical and systematic, respectively. Bottom: Differential production cross sections of $d\sigma(B^+)/dp_T(B^+) \times \mathcal{B}(B^+ \rightarrow J/\psi K^+)$ and $d\sigma(B^+)/d|y|(B^+) \times \mathcal{B}(B^+ \rightarrow J/\psi K^+)$ at $\sqrt{s}$= 7 TeV pp collisions. Solid points with uncertainty bar are the CMS measurements and the uncertainties are statistical and systematic, respectively. The shaded region shows the theoretical uncertainty due to the mass of the b-quark, renormalization and factorization scales. The ratio of the measurement to the predictions from FONLL is shown in the lower part of the plots.

References

[1] P. Nason, S. Dawson and R.K. Ellis, ”The total cross section for the production of heavy quarks in hadronic collisions”, Nucl. Phys. **B 303** (1988) 607.

[2] P. Nason, S. Dawson and R.K. Ellis, ”The one particle inclusive differential cross section for heavy quark production in hadronic collisions”, Nucl. Phys. **B 327** (1989) 49 [Erratum ibid. **B 335** (1990) 260].

[3] M. Cacciari, M. Greco and P. Nason, ”The p_T spectrum in heavy flavor hadroproduction”, JHEP **05** (1998) 007 [hep-ph/9803400].

[4] M. Cacciari, S. Frixione and P. Nason, ”The p_T spectrum in heavy flavor photoproduction”, JHEP 03 (2001) 006 [hep-ph/0102134].

[5] Quarkonium Working Group collaboration, ”Heavy quarkonium physics”, (2004). arXiv:hep-ph/0412158, and references therein.

[6] C.-H. Chang and Y.-Q. Chen, ”Hadronic production of the Bc meson at TeV energies”, Phys. Rev. D **48**, 4086 (1993).

[7] Chao-Hsi Chang *et al.*, ”On hadronic production of the B_c meson”, Phys. Lett. B**364**:78-86 (1995).

[8] Chao-Hsi Chang *et al.*, ”The Projection scheme for handling large number cancellation related to gauge invariance”, Phys. Rev. D **54**, 6963 (1996).

[9] C.-H. Chang, C.-F. Qiao, J.-X. Wang, and X.-G. Wu, ”Color-octet contributions to P-wave Bc meson hadroproduction”, Phys. Rev. D **71**, 074012 (2005).

[10] K. Kolodziej, A. Leike, and R. Ruckl, ”Production of Bc mesons in hadronic collisions”, Phys. Lett. B **355**, 337 (1995).

[11] A. V. Berezhnoy, A. K. Likhoded, and M. V. Shevlyagin, ”Hadronic production of Bc mesons”, Phys. At. Nucl. **58**, 672 (1995).

[12] A. V. Berezhnoy, V. V. Kiselev, and A. K. Likhoded, ”Photonic production of S- and P-wave Bc states and doubly heavy baryons”, Z. Phys. A **356**, 89 (1996).

[13] S. P. Baranov, ”Pair production of $B_c^{(*)}$ mesons in p-p and $\gamma\gamma$ collisions”v, Phys. Rev. D **55**, 2756 (1997).

[14] C.-H. Chang and X.-G. Wu, ”Uncertainties in estimatin hadronic production of the meson B_c and comparisons between TEVATRON and LHC”, Eur. Phys. J. **C38**(2004) 267, arXiv:hep-ph/0309121.

[15] Y.-N. Gao, J.-B. He, P. Robbe, M.-H. Schune, and Z.-W. Yang, ”Experimental prospects of the B_c studies of the LHCb experiment”, Chin. Phys. Lett. **27**, 061302 (2010).

[16] UA1 collaboration, C. Albajar *et al.*, ”Beauty production at the CERN proton-anti-proton collider”, Phys. Lett. **B 186** (1987) 237.

[17] UA1 collaboration, C. Albajar *et al.*, ”Measurement of the bottom quark production cross section in proton-anti-proton collisions at $\sqrt{s} = 0.63$ TeV”, Phys. Lett. **B 213** (1988) 405.

[18] CDF collaboration, ”Measurement of the bottom quark production cross section using semileptonic decay electrons in $p\bar{p}$ collisions at $\sqrt{s} = 1.8$ TeV”, Phys. Rev. Lett. **71** (1993) 500-504. doi:10.1103/PhysRevLett.71.500.

[19] CDF collaboration, ”Measurement of the B meson differential cross-section, $d\sigma/dp_T$”, in $p\bar{p}$ collisions at $\sqrt{s} = 1.8$ TeV, Phys. Rev. Lett. **75** (1995) 1451-1455. doi:10.1103/PhysRevLett.75.1451.

[20] CDF collaboration, ”Measurement of the B^+ total cross section and B^+ differential cross section $d\sigma/dp_T$ in $p\bar{p}$ collisions at $\sqrt{s} = 1.8$ TeV”, Phys. Rev. **D65** (2002) 052005. doi:10.1103/PhysRevD.65.052005.

[21] CDF collaboration, ”Measurement of the J/ψ meson and b-hadron production cross sections in $p\bar{p}$ collisions at $\sqrt{s} = 1960$ GeV”, Phys. Rev. **D71** (2005) 032001. doi:10.1103/PhysRevD.71.032001.

[22] CDF collaboration, ”Measurement of the B^+ production cross section in $p\bar{p}$ collisions at $\sqrt{s} = 1960$ GeV”, Phys. Rev. **D75** (2007) 012010. doi:10.1103/PhysRevD.75.012010.

[23] D0 collaboration, ”Inclusive μ and B quark production cross-sections in $p\bar{p}$ collisions at $\sqrt{s} = 1.8$ TeV”, Phys. Rev. Lett. **74** (1995) 3548-3552. doi:10.1103/PhysRevLett.74.3548.

[24] D0 collaboration, ”Small angle muon and bottom quark production in $p\bar{p}$ collisions at $\sqrt{s} = 1.8$ TeV”, Phys. Rev. Lett. **84** (2000) 5478-5483. doi:10.1103/PhysRevLett.84.5478.

[25] D0 collaboration, ”Cross section for b jet production in $p\bar{p}$ collisions at $\sqrt{s} = 1.8$ TeV”, Phys. Rev. Lett. 85 (2000) 5068(C5073. doi:10.1103/PhysRevLett.85.5068.

[26] CDF collaboration, ”Observation of the B_c meson in $p\bar{p}$ collisions at $\sqrt{s} = 1.8$ TeV”, Phys. Rev. Lett. **81**, 2432 (1998),

[27] CDF Collaboration, ”Observation of the B_c meson in $p\bar{p}$ collisions at $\sqrt{s} = 1.8$ TeV”, Phys. ReV. D**58**, 112004 (1998).

[28] CDF collaboration, ”Observation of the Decay $B_c^{\pm} \to J/\psi\pi^p m$ and Measurement of the $B_c^{\pm}$ Mass”, Phys. Rev. Lett., **100**, 182002 (2008).

[29] D0 collaboration, ”Observation of the B_c Meson in the Exclusive Decay $B_c \to J/\psi\pi$”, Phys. Rev. Lett. **101**, 012001 (2008).

[30] LHCb collaboration, ”Measurement of the $B^{\pm}$ production cross-section in pp collisions at $\sqrt{s} = 7$ TeV”, JHEP **04** (2012) 093.

[31] LHCb collaboration, ”Measurement of $\sigma(pp \to b\bar{b}X)$ at $\sqrt{s} = 7$ TeV in the forward region”, Phys. Lett. **B 694** (2010) 209.

[32] LHCb Collaboration, ”Measurements of B_c^+ production and mass with the $B_c^+ \to J/\psi\pi^+$ decay”, Phys. Rev. Lett. **109**, 232001 (2012).

[33] LHCb Collaboration, ”First observation of the decay $B_c \to J/\psi\pi^+\pi^-\pi^+$”, Phys. Rev. Lett. **108**, 251802 (2012).

[34] LHCb Collaboration, ”Measurements of B_c^+ production Production in Proton-Proton Collisions at $\sqrt{s} = 8$ TeV”, Phys. Rev. Lett. **114**, 132001 (2015).

[35] CMS collaboration, "Measurement of the B^+ production cross section in pp collisions at $\sqrt{s} = 7$ TeV", Phys. Rev. Lett. **106** (2011) 112001.

[36] CMS collaboration, "B^0 Production Cross Section in pp Collisions at $\sqrt{s} = 7$ TeV", Phys. Rev. Lett. **106** (2011) 252001.

[37] CMS collaboration, "Measurement of the strange B meson production cross section with $J/\psi\phi$ decays in pp collisions at $\sqrt{s} = 7$ TeV", Phys. Rev. **D 84** (2011) 052008.

[38] CMS collaboration, "Measurement of the Λ_b cross section and the $\bar{\Lambda}_b$ to Λ_b ratio with Λ_b to $J/\psi\Lambda$ decays in pp collisions at $\sqrt{s} = 7$ TeV", Phys. Lett. **B 714** (2012) 136.

[39] CMS collaboration, "Inclusive b-hadron production cross section with muons in pp collisions at $\sqrt{s} = 7$ TeV", JHEP **03** (2011) 090.

[40] CMS collaboration, "Measurement of the cross section for production of $b\bar{b}\ X$ decaying to muons in pp collisions at $\sqrt{s} = 7$ TeV", JHEP 06 (2012) 110.

[41] CMS collaboration, "Inclusive b-jet production in pp collisions at $\sqrt{s} = 7$ TeV", JHEP **04** (2012) 084.

[42] CMS Collaboration, "Measurement of the ratio of the production cross section times branching fraction between the $B_c \to J/\psi\pi$ and the $B^+ \to J/\psi K$ and of branching fractions $B_c \to J/\psi\pi\pi\pi$ over $B_c \to J/\psi\pi$ in CMS at $\sqrt{s} = 7$ TeV", JHEP **1501** (2015) 063.

[43] ATLAS collaboration, "Measurement of the b-hadron production cross section using decays to $D^{\star}\mu^- X$ final states in pp collisions at $\sqrt{s} = 7$ TeV with the ATLAS detector", Nucl. Phys. **B 864** (2012) 341.

[44] ATLAS collaboration, "Measurement of the inclusive and dijet cross-sections of b-jets in pp collisions at $\sqrt{s} = 7$ TeV with the ATLAS detector", Eur. Phys. J. **C 71** (2011) 1846.

[45] ATLAS collaboration, "Measurement of the differential cross-section of B^+ meson production in pp collisions at $\sqrt{s} = 7$ TeV at ATLAS", JHEP **10** (2013) 042.

[46] CMS collaboration, "The CMS experiment at the CERN LHC", JINST **3** (2008) S08004, doi:10.1088/1748-0221/3/08/S08004.

[47] J. Chang, C Wang and X.Wu, BCVEGPY2.0: "An upgraded version of the generator BCVEGPY with the addition of hadroproduction of the P-wave B_c states", Comput.Phys.Communication 174 (2006) 11, doi:10.1016/j.cpc.2005.09.008.

[48] Sjostrand, Torbjorn and Mrenna, Stephen and Skands, Peter Z., "PYTHIA 6.4 Physics and Manual", JHEP05 (2006) 026.

[49] Chao-Hsi Chang, Jian-Xiong Wang and Xing-Gang Wu, "An Upgraded version of the generator BCVEGPY2.0 for hadronic production of B(c)meson and its excited states", Comput.Phys. Commun. **175**, 624 (2006).

[50] C. Patrignani *et al.*, "Particle Data Group", Chin. Phys. C, 40, 100001 (2016).

[51] G.E. Forden and D.H. Saxon, "Improving vertex position determination using a kinematic fit" , Nucl. Instrum. Meth. A 248 (1986) 439

[52] CMS collaboration, "Measurement of Tracking Efficiency", CMS Physics Analysis Summary CMS-PAS-TRK-10-002, 2010. `https://cds.cern.ch/record/1279139`

[53] CMS Collaboration, "Absolute Calibration of Luminosity Measurement at CMS: Summer 2011 Update", CMS Physics Analysis Summary CMS-PAS-EWK-11-001, 2011. `https://cds.cern.ch/record/1376102`

[54] C.-F. Qiao, P. Sun, D. Yang, and R.-L. Zhu, "B_c exclusive decays to charmonium and a light meson at next-to- leading-order accuracy", Phys.Rev. **D**89 034008 (2014).

[55] C. Chang, C. Driouchi, P. Eerola, and X.Wu, "BCVEGPY: an event generator for hadronic production of the B_c meson", Comput.Phys.Communication 159 (2004) 33, doi:10.1016/j.cpc.2004.02.005

[56] Chao-Hsi Chang *et al.*, "Hadronic Production of the P-wave excited B_c states $B^*(cJ, L = 1)$", Phys. Rev. D**70**:114019(2004); Chao-Hsi Chang *et al.*, "The color-octet contributions to P-wave B_c meson hadron production", Phys. Rev. D**71**:074012(2005).

[57] C. F. Qiao and R. L. Zhu, "Estimation of semileptonic decays of B_c meson to S-wave charmonia with nonrelativistic QCD", Phys. Rev. D **87**, 014009 (2013).

[58] M. Cacciari, S. Frixione, N. Houdeau, M. L. Mangano, P. Nason and G. Ridolfi, "Theoretical predictions for charm and bottom production at the LHC", JHEP **1210** (2012) 137 [arXiv:1205.6344 [hep-ph]].

[59] J. M. Shen, et al., "QCD corrections to the B_c to charmonia semileptonic decay", Phys. Rev. D **90**, 034025 (2014).

[60] S. J. Brodsky and X. G. Wu, Phys. Rev. D**85**, 034038 (2012); S. J. Brodsky and X. G. Wu, Phys. Rev. Lett. **109**, 042002 (2012); M. Mojaza, S. J. Brodsky and X. G. Wu, Phys. Rev. Lett. **110**, 192001 (2013); S. J. Brodsky, M. Mojaza and X. G. Wu, Phys. Rev. D**89**, 014027 (2014).